

Published in final edited form as:

Acta Biomater. 2014 February ; 10(2): 785–791. doi:10.1016/j.actbio.2013.09.025.

Elastic modulus and collagen organization of the rabbit cornea: epithelium to endothelium

Sara M. Thomasy^a, Vijay Krishna Raghunathan^a, Moritz Winkler^b, Christopher M. Reilly^c, Adeline R. Sadeli^a, Paul Russell^a, James V. Jester^b, and Christopher J. Murphy^{a,d,*}

^aDepartment of Surgical and Radiological Sciences, School of Veterinary Medicine, University of California-Davis, Davis, CA 95616.

^bDepartment of Biomedical Engineering, University of California-Irvine, Irvine, California, USA.

^cDepartment of Pathology, Immunology and Microbiology, School of Veterinary Medicine, University of California-Davis, Davis, CA 95616.

^dDepartment of Ophthalmology and Vision Science, School of Medicine, University of California-Davis, Davis, CA 95616.

Abstract

The rabbit is commonly used to evaluate new corneal prosthetics and study corneal wound healing. Knowledge of the stiffness of the rabbit cornea would better inform design and fabrication of keratoprosthesis and substrates with relevant mechanical properties for *in vitro* investigations of corneal cellular behavior. This study determined the elastic modulus of the rabbit corneal epithelium, anterior basement membrane (ABM), anterior and posterior stroma, Descemet's membrane (DM) and endothelium using atomic force microscopy (AFM). In addition, three-dimensional collagen fiber organization of the rabbit cornea was determined using nonlinear optical high-resolution microscopy. Elastic modulus as determined by AFM for each corneal layer was: epithelium 0.57 ± 0.29 kPa (mean \pm SD), ABM 4.5 ± 1.2 kPa, anterior stroma 1.1 ± 0.6 kPa, posterior stroma 0.38 ± 0.22 kPa, DM 11.7 ± 7.4 kPa, and endothelium 4.1 ± 1.7 kPa. Biophysical properties, including elastic modulus, are unique for each layer of the rabbit cornea and are dramatically softer in comparison to the corresponding regions of the human cornea. Collagen fiber organization is also dramatically different between the two species with markedly less intertwining observed in the rabbit versus human cornea. Given that substratum stiffness considerably alters corneal cell behavior, keratoprosthesis that incorporate mechanical properties simulating the native human cornea may not elicit optimal cellular performance in rabbit corneas that have dramatically different elastic moduli. These data will allow for the design of substrates that better mimic the biomechanical properties of the corneal cellular environment.

© 2013 Acta Materialia Inc. Published by Elsevier Ltd. All rights reserved.

*Corresponding author. Tel. 530-752-0926, Fax. 530-752-3708 cjmurphy@ucdavis.edu.

Publisher's Disclaimer: This is a PDF file of an unedited manuscript that has been accepted for publication. As a service to our customers we are providing this early version of the manuscript. The manuscript will undergo copyediting, typesetting, and review of the resulting proof before it is published in its final citable form. Please note that during the production process errors may be discovered which could affect the content, and all legal disclaimers that apply to the journal pertain.

Conflicts of Interest

The authors have no conflicts of interest.

Keywords

cornea; elastic modulus; AFM; nonlinear optical high-resolution microscopy; rabbit

1. Introduction

The cornea functions as a protective barrier while simultaneously transmitting and refracting light at the anterior aspect of the eye. In order to complete these diverse functions, the human cornea is composed of six different histologic layers, each with a unique structure - the epithelium, anterior basement membrane, Bowman's layer, stroma, Descemet's membrane, and endothelium. The regenerative, stratified, nonkeratinized anterior epithelium consists of superficial squamous, polygonal wing and a single layer of columnar basal cells. The basal cells participate in the elaboration of an anterior basement membrane, a specialized extracellular matrix comprised of specific proteins and possessing a complex three-dimensional architecture. Bowman's layer is a thin, acellular zone of compacted collagen fibers that resides subjacent to the anterior epithelium and its associated basement membrane. It is absent in all non-primate laboratory animals including rabbits. The bulk of the corneal thickness (approx. 90%) is attributable to the stroma, which is comprised of sheet-like, fibrillar, parallel bundles of collagen and a sparse population of interconnected keratocytes located between the lamellae. Descemet's membrane, similar to the anterior basement membrane, is a specialization of the extracellular matrix that connects the endothelial cells to the underlying stroma. The endothelium is comprised of a single layer of hexagonal cells that participate in the production of Descemet's membrane. In addition to each layer possessing a distinct structure and chemical composition, the biomechanical properties of each layer are also unique.

Our group has previously reported the local elastic modulus of the human corneal basement membranes, anterior stroma and Bowman's layer as determined by atomic force microscopy (AFM). [1, 2]. Interestingly, the elastic modulus for the more compact Descemet's membrane was greater than the anterior basement membrane at 47 and 8 kPa, respectively [1]. A similar observation was found for the more compact Bowman's layer in comparison to the anterior stroma with elastic moduli of 110 and 33 kPa, respectively [2]. Despite the wide use of the rabbit to study corneal biology and wound healing, as well as in the development of ocular therapeutics and devices, the biophysical attributes of the rabbit cornea have not been fully characterized. Specifically, only the bulk elastic modulus of rabbit corneas have been reported prior to and following photodynamic cross-linking at 11 and 20 MPa, respectively, using tensile testing [3]. As indicated in a recent review article, elastic modulus values are strongly dependent on the testing method employed and values obtained by tensile testing do not directly correlate with values obtained using AFM [4]. Knowledge of the elastic modulus of the rabbit cornea would inform design and fabrication of biomimetic substrates in order to improve the relevance of results obtained from *in vitro* investigations and provide critical data for development of keratoprosthetics with enhanced performance. Thus, the purposes of this study were 1) to determine the elastic modulus of the epithelium, anterior basement membrane, anterior and posterior stroma, Descemet's membrane and endothelium of the rabbit cornea, 2) to characterize the collagen fiber

organization of the rabbit cornea in three dimensions using nonlinear optical high-resolution microscopy (NLO-HRMac) and correlate these findings with the biomechanical data and 3) to determine the influence of storage in Optisol, a commercially available preservative commonly used for human donor corneal tissue, on the elastic modulus of the rabbit corneal layers.

2. Methods

2.1 Animals

Sixteen Dutch Belted female rabbits (Covance, Princeton, NJ) with a mean \pm SD body weight and age of 2.1 ± 0.2 kg and 1.1 ± 0.2 years, respectively, were utilized in this study. All aspects of the study were approved by the Institutional Animal Care and Use Committee of the University of California-Davis and were performed according to the Association for Research in Vision and Ophthalmology resolution on the use of animals in research. A complete ophthalmic examination (slit lamp examination & indirect ophthalmoscopy), applanation tonometry (Tonopen XL, Medtronic, Minneapolis, MN), ultrasonic pachymetry (Accupach VI, Accutome, Malvern, PA), and fluorescein staining were performed prior to harvesting the corneas. Only animals free of ocular disease were included in the study.

To obtain the epithelium, endothelium, anterior basement membrane and Descemet's membrane, rabbits were euthanized with pentobarbital (200 mg/kg, IV) and an 8 mm central corneal button was harvested from both eyes using a corneal trephine and corneal section scissors. For measurement of epithelial and endothelial layers, the corneal buttons were divided into 2 mm sections and stored in Optisol (Chiron Ophthalmics, Irvine, California) at 4° C until measurements were performed (storage times provided below). For the anterior basement membrane and Descemet's membrane, the epithelial and endothelial cells were removed, respectively, using a modification of previously reported procedures [5]. Briefly, epithelial cells were removed by placing the corneas in 2.5 mM ethylenediamine tetraacetic acid (EDTA) in HEPES buffer (pH = 7.2) for 2.5 hours at 37° C followed by sonication (Crest Ultrasonic Cleaner, WI, USA) at 2 amps for 5 minutes. The endothelium was removed by placing the corneas in the EDTA solution for 30 minutes at 37° C followed by sonication (Crest Ultrasonic Cleaner) at 2 amps for 5 minutes. For the anterior and posterior stroma, the rabbits were sedated with xylazine and ketamine and the epithelial cells were removed with an excimer spatula (BD Visitec, Franklin Lakes, NJ, USA). An excimer laser (Nidek Excimer Laser Corneal Surgery System EC-5000, Fremont, CA) was used to photoblade the superficial stromal elements of the cornea to expose anterior stroma (1 cycle of 6 mm diameter, 40 Hz, 167 pulses, 100 μ m depth) and posterior stroma (2 cycles at 6 mm diameter, 40 Hz, 208 pulses, 125 μ m depth - i.e. 250 μ m total depth) as central corneal thickness in rabbits is typically 350 μ m [6]. The corneas were stored in Optisol at 4° C until AFM measurements could be performed and the left or right eye from each rabbit was randomly assigned to incubate in Optisol for <2 h or 24 h. For the measurement, tissues were adhered using cyanoacrylate glue in the center of an AFM dish (World Precision Instruments, FL, USA). AFM analysis was performed in 1 \times Dulbecco's phosphate buffered saline (DPBS). A 2 mm corneal section was also placed in 10% formalin for histologic examination to confirm that the layer of interest was intact and exposed for AFM analysis.

These corneal sections were fixed in 10% neutral buffered formalin (Bausch & Lomb, Rochester, NY), embedded in paraffin, sectioned at 5 μm , and stained with hematoxylin and eosin (all sections) and Periodic acid-Schiff (ABM only).

2.2 AFM Contact Mechanics

Prior to analysis, the samples were equilibrated in Dulbecco's phosphate buffered saline (pH 7.4) at room temperature for 2–3 h to eliminate thermal drift. Silicon nitride cantilevers (PNP-TR-50, length = 100 μm , actual $k = 55 - 246$ pN/nm, Nano World, Switzerland) incorporated with rigid spheres (Dry Borosilicate Glass Microspheres, actual radius = 4.6 – 5.9 μm , Thermoscientific, Fremont, CA, USA) on their conical tip were used for AFM after UV sterilization (UV/Ozone Procleaner, BioForce Nanoscience, Ames, IA) for 1 h to effectively remove organic contaminants. Spring constant of each cantilever probe, used for indentation measurements, were determined and calibrated by performing thermal tuning, a measure of the cantilever's response to thermal noise. Deflection sensitivity of the probes was obtained by taking the average of 5 force curves on a glass slide in DPBS.

The elastic modulus (E) of each sample was obtained by fitting indentation force versus indentation depth of the sample with an overlay of the theoretical force based on the Hertz model as shown in equation 1 for spherical tip geometry.

$$F = \frac{4}{3} \frac{E}{1 - \nu^2} \delta^{\frac{3}{2}} R^{\frac{1}{2}} \quad (1)$$

Where F is the force applied by the indenter, E is Young's modulus, ν is Poisson's ratio (assumed to be 0.5 for biological tissues [7]), δ is indentation depth, and R is radius of the tip. The bulk properties of biological tissues are classically viscoelastic, heterogenous and not infinitely thick. However, in order to use AFM to determine the mechanical properties of biological tissues, we assume that the sample is linearly elastic, homogenous, incompressible and infinitely thick up to a limited indentation depth. Determining the accurate indentation depth across which the biological tissue sample behaves as elastic is difficult from the force (F) versus indentation depth (δ) curve. Thus the elastic regime of a viscoelastic tissue, where E is constant over a restricted indentation depth, was determined from a plot of elastic modulus (E) versus δ values (Fig. 1). Contact point was visually detected where the cantilever's deflection deviated from the zeroed deflection. For each sample, 5 single force curves at 2 $\mu\text{m/s}$ were taken at 5 different locations around the center of the sample. In addition, many curves were averaged together to produce mean and standard deviation force vs. indentation plots (Figure 2). This plot shows 25 different indentation vs. force curves (gray dots) measured at multiple positions on the endothelium from one rabbit. At each indentation depth, the average and standard deviation of the 25 curves were calculated (blue lines). From these curves, a single curve of the average and two additional curves of the positive and negative standard deviations were generated (black lines). A linear least-squares fit of the data using the Hertz model was then performed to the elastic region of the average, positive and negative standard deviations to give an overall average and standard deviation of the elastic modulus.

2.3 NLO-HRMac Sample Preparation

Rabbit eyes were acquired from Pel-Freez Biologicals (Rogers, AR) and were partially immersed in cell culture media (Dulbecco's Modified Eagle Media, Gibco Life Technologies, Grand Island, NY) and placed in an incubator at 37°C for 45 minutes to temporarily restore endothelial pump function. After partial clearing of corneal edema was observed, intraocular pressure (IOP) was increased to 50 mmHg by infusing phosphate buffered saline solution (PBS, pH 7.4) for 30 min in order to drive water out of the corneas and to mechanically load and straighten collagen fibers. Eyes were then fixed under pressure by perfusion with 4% paraformaldehyde (Electron Microscopy Science, Hartfield, PA) in PBS. This procedure served to decrease post-mortem swelling and fiber crimping due to lack of load following post-mortem IOP decrease. Finally, a corneoscleral button was dissected from each globe using a scalpel blade, and the corneas were cut in two sections from limbus to limbus. The larger section was embedded vertically in low melting point agarose (NuSieve GTG, Lonza, Rockland, ME). A vibratome (Vibratome 1500, Intracel Ltd, Shepreth, UK) was used to cut multiple, consecutive, approximately 300 μm thick sections which were stored in PBS.

2.4 NLO-HRMac Imaging and Image Processing

Cornea cross-sections were imaged following previously established methods [8]. Briefly, sections were scanned using a Zeiss 510 LSM Meta microscope (Carl Zeiss Inc., Thornwood, NY) using 820nm, 150fs laser pulses. Forward- and backscattered second harmonic generation light was collected as two separate channels. Several hundred consecutive overlapping image stacks were acquired using a 20 \times /0.7 NA (low-resolution overview, 0.88 $\mu\text{m}/\text{px}$) and a 40 \times /1.2 NA (high-resolution 3-D region reconstruction, 0.44 $\mu\text{m}/\text{px}$) objective. Each image stack consisted of multiple optical planes down to a depth of approximately 120 μm .

Image data were exported as individual TIFF files and individual images were stitched using custom-written ImageJ scripts to form a single, large-scale, high-resolution mosaic. For three-dimensional reconstruction, mosaics were loaded into Amira 5.4 (Visage Imaging, Carlsbad, CA). Representative collagen fibers in the anterior, mid and posterior stroma were individually segmented using the label field module by manually highlighting them across adjacent slices. Segmented fiber populations were then rendered in 3-D using the surface render module.

2.5 Statistical Analysis

A paired difference *t* test was used to assess differences in intraocular pressure and central corneal thickness between left and right eyes as well as to determine the effects of incubation time in Optisol on elastic modulus for each corneal layer. Significance was set at $P < 0.05$ for all analyses. All data are presented as mean \pm SD.

3. Results

All corneas appeared healthy and free of disease following ophthalmic examination and no corneas retained fluorescein stain indicating an intact epithelium. Mean (\pm SD) intraocular

pressure was $15.9 \pm 4.8 \mu\text{m}$ and $16.6 \pm 4.8 \mu\text{m}$ for the left and right eyes, respectively and there was no significant difference ($P = 0.38$) between the two eyes. Mean (\pm SD) central corneal thickness was $364 \pm 17 \mu\text{m}$ and $360 \pm 14 \mu\text{m}$ for the left and right eyes, respectively and there was no significant difference ($P = 0.49$) between the two eyes. Histologic examination of specimens not used in AFM analysis confirmed that the layer of interest was intact and exposed. For each sample that was photoablated to expose the anterior or posterior stroma, there was no difference in stromal characteristics at the edges of the stromal defect, compared to the stroma deep and adjacent to the defect margins.

3.1. Epithelium and endothelium

Elastic modulus versus indentation depth curves showed that the elastic modulus was relatively constant over indentation depths of 50 to 200 nm for the rabbit corneal epithelium and endothelium (Fig. 1). For the day 0 samples, the mean \pm SD elastic modulus was 0.57 ± 0.29 kPa and 4.1 ± 1.7 kPa (Fig. 3) for the epithelium and endothelium, respectively. Incubation in Optisol for 24 h did not have a significant effect ($P = 0.95$) on the elastic modulus of the epithelium (0.56 ± 0.27 kPa). Incubation in Optisol for 24 h also did not have a significant effect ($P = 0.47$) on the elastic modulus of the endothelium (6.8 ± 6.3 kPa) but there was more variability between the samples at day 1 in comparison to day 0 as evidenced by the larger standard deviation.

3.2 Anterior and posterior stroma

Force curves were obtained after photoablation to determine the elastic modulus of the anterior and posterior corneal stroma. The mean elastic modulus was 1.1 ± 0.6 kPa and 0.38 ± 0.22 kPa for anterior and posterior stroma, respectively, on day 0 (Fig. 3). There was no significant effect ($P = 0.88$ or $P = 0.31$, respectively) of incubation in Optisol for 24 h on the elastic modulus of the anterior stroma (0.95 ± 0.68 kPa) or posterior stroma (0.42 ± 0.27 kPa).

The collagen fiber organization of the rabbit cornea is demonstrated in this low resolution ($0.88 \mu\text{m}/\text{pixel}$), single-plane NLO-HRM image of a single section from the central corneal meridian of a rabbit cornea cut in superior-inferior direction (Fig 4). Note the heterogeneity in collagen fiber interactions present within the axial anterior cornea in a high-resolution ($0.44 \mu\text{m}/\text{pixel}$) single-plane region of the central rabbit cornea (Fig 4 inlay). A three dimensional reconstruction of the central rabbit cornea demonstrates that the majority of the rabbit cornea exhibits parallel arrangement of collagen fibers (Supplementary Video 1). The collagen fiber arrangement of the rabbit cornea markedly differs from the human cornea which has extensive collagen fiber intertwining in the anterior 80% (Fig 5).

3.3. Anterior basement membrane and Descemet's membrane

The value obtained for the elastic modulus of the anterior basement membrane was 4.5 ± 1.2 kPa, while the modulus obtained for Descemet's membrane was 11.7 ± 7.4 kPa (Fig. 3). Incubation in Optisol for 24 h did not have a significant effect ($P = 0.38$ or $P = 0.42$, respectively) on the elastic modulus of the anterior basement membrane (6.5 ± 2.3 kPa) or Descemet's membrane (17.8 ± 5.6 kPa).

4. Discussion

This study determined the local stiffness of six distinct spatial regions of the rabbit cornea using AFM nanoindentation. We chose to use a spherical AFM tip with a radius of approximately 5 microns to minimize the strain field and to ensure that the tip size was larger than that of topographic features observed in the corneal stroma and membranes. There was some variability in elastic modulus between individuals at all corneal locations despite the rabbits being the same breed, gender and of similar age. This variation is expected given the challenges associated with measuring the elastic modulus of soft, biologic tissues [4]. Incubation in Optisol for 24 h did not have a significant impact on the elastic modulus of any corneal layer. Thus, the data generated in the present study of elastic modulus in the rabbit cornea can be directly compared with previous measurements of elastic modulus in the human cornea using AFM [2]. Indeed, all three layers that could be directly compared between the two species, anterior basement membrane, anterior stroma, and Descemet's membrane, were markedly stiffer in the human cornea in comparison to the rabbit cornea [2]. Using NLO-HRMac imaging, we were able to demonstrate that the collagen organization dramatically differs between the rabbit and human cornea and that this likely contributes to the observed differences in stromal biomechanics.

In both species, Descemet's membrane is stiffer than the anterior basement membrane but the difference in elastic modulus between these basement membranes is more dramatic in humans versus rabbits at 8 and 2.5-fold, respectively [9]. In the human cornea, Descemet's membrane appears to be more compact than the anterior basement membrane due to a smaller average pore diameter (more compact 3-dimensional organization) and this structural difference is likely responsible for the difference in elastic modulus between these basement membranes [5]. While the topographic features of rabbit basement membranes have not been investigated, the canine Descemet's membrane also demonstrates a smaller average feature size in comparison to the anterior basement membrane [10]. Thus, this difference may be generalizable to the mammalian cornea where the more compact Descemet's membrane results in a greater elastic modulus in comparison to the more porous and thus softer anterior basement membrane. Descemet's membrane increases in thickness with age and the elastic properties may be modulated throughout the life of the individual. The rabbits were young healthy individuals less than 1 year of age whereas the human corneas investigated were from middle aged to older individuals (58–72 years) [9]. The underlying reasons for the differences in architecture have not been thoroughly investigated, though we note that the anterior basement membrane supports a relatively labile epithelial covering with constant migration and associated remodeling activities whereas the endothelial population is relatively static.

The elastic modulus of the rabbit corneal endothelium was approximately 8-fold greater than the epithelium. This difference is likely due to intrinsic differences in the cytoarchitecture of the differing cell types as well as possible contributions from a substratum effect. It has been previously demonstrated that cellular stiffness is profoundly influenced by and the stiffness for a given cell type parallels the stiffness of the underlying substrate [11]. In other words, cells assume a stiffer profile when cultured on stiffer substrates. This substratum effect would be more pronounced in the corneal endothelium since it is only one layer thick in

comparison to the epithelium which is several layers thick in the rabbit. The most superficial corneal epithelial cells are flat, desquamating, and contain degenerating mitochondria [12]. In contrast, corneal endothelial cells are cuboidal and are densely packed with abundant mitochondria and a prominent endoplasmic reticulum [12].

The present study demonstrated that the rabbit anterior stroma had an approximately 3-fold greater elastic modulus in comparison to the posterior stroma. This is similar to a recent study investigating the elastic modulus of the human cornea which reported a 2.2-fold greater elastic modulus in the anterior stroma in comparison to the posterior stroma [8]. This finding was attributed to increased collagen intertwining within the anterior versus posterior stroma in the human cornea. Using NLO-HRMac imaging, we also demonstrated increased collagen fiber intertwining in the anterior stroma of the rabbit cornea while the posterior stroma exhibited a parallel collagen fiber arrangement. This observation is consistent with a recent investigation of corneal stromal structure in several species which demonstrated strong interwoven collagen organization in the anterior stroma of the rabbit cornea while the posterior stroma had longer collagen bundles predominantly oriented parallel to the corneal surface [13]. In addition, it has been shown that keratocyte density is greater in the anterior stroma in comparison to the posterior stroma of several species including rabbits [6]. Thus, the difference in elastic modulus observed in the rabbit anterior and posterior stroma is likely due to structural variations in collagen organization and differences in keratocyte density between these two regions.

Similar to the corneal basement membranes, the anterior stroma of the human cornea is markedly stiffer in comparison to the rabbit cornea with elastic moduli of 33 and 1.1 kPa, respectively [2]. Using NLO-HRMac imaging, we also demonstrated marked differences in collagen fiber arrangement between rabbit and human stroma that likely contribute to the difference in elastic modulus between the two species. Specifically, we demonstrated that only the most anterior portion of the rabbit stroma exhibits collagen fiber intertwining with the bulk of the stroma possessing a parallel collagen fiber arrangement. This architecture markedly contrasts with the human stroma where the anterior 80% of the stroma demonstrates extensive collagen fiber interweaving with a parallel arrangement of the collagen fibers only in the posterior 20% of the stroma [8]. However, there are also some key differences between the previous study of human corneas [2] and the present study which may partially account for the 30-fold difference in elastic moduli between the two species. First, the depth of measurement of the stroma was more anterior in the previous study (20 μm) in comparison to the present study (100 μm) [2], especially when considering that human central corneal thickness is greater than rabbits at 500 versus 350 μm , respectively [6]. Winkler and colleagues demonstrated increased collagen intertwining and crosslinking present within the anterior stroma just underlying Bowman's layer [8] and this finding may be partially responsible for the greater elastic modulus observed in the human cornea. Bowman's layer is present in some species including the human but is not present in the rabbit. In addition, the rabbits in the present study were young adults while the previous study was primarily comprised of older humans [2]. The human cornea has been shown to stiffen with age [14, 15] and part of the difference in elastic moduli reported for the rabbit and human anterior stroma might be attributed to the age of the cornea. Nevertheless, there are dramatic differences in surgical tissue handling properties between rabbit and human

cornea and it is not surprising that the stroma, which comprises the bulk of the cornea, is markedly stiffer in humans in comparison to rabbits. Given that substratum stiffness plays a critical role in the modulation of cell behavior [16–18], keratoprosthetics that incorporate biomechanical features from one species may behave much differently in a different species with a markedly different corneal elastic moduli. Thus, it may be worthwhile to investigate the elastic moduli of the corneal stroma in other species used in keratoprosthetic design development, such as dogs, to determine if their biomechanical properties more closely approximate that of the human corneal stroma.

One of the practical considerations employed in this study was the requirement of the excimer laser to create a homogenous stromal surface with a precise depth in order to obtain force curves with AFM. This method was chosen in order to obtain exquisite, repeatable control of depth and to enable comparison of results obtained for the rabbit with those reported for the human corneal stiffness profile that also employed excimer photoablation to expose defined depths with the stroma [2]. We recognize that the use of an excimer laser is capable of altering the corneal surface [19]. Studies detailing the thermodynamic dependent modulation of viscoelastic properties of soft tissues demonstrate heat induced increases in hysteresis and compliance accompanied by shrinkage of tissue or curling of collagen fibers [20]. Importantly, these changes depended on the extent of prior thermal damage rather than the thermo-mechanical method that induced the damage. Furthermore, the ultraviolet laser ablation induced by an excimer laser on soft biological tissues like the cornea is a surface-mediated rather than explosive mechanical process [21]. In this study, histology showed a precise stromal defect with no curling or artifactual damage to the stroma with the use of an excimer laser. While recognizing the caveats inherent to photoablation, the results obtained using identical techniques document significant differences throughout the stromal thickness as well as markedly different values between the human and rabbit. We thus speculate that the photoablation had little inadvertent effect on the gross structure or biomechanical properties of the corneal stroma. We also note the anterior stroma was exposed using an excimer laser in the previous study by evaluating the elastic modulus of the human cornea with AFM [2] so the results in the present study are directly comparable. Additionally, it must be carefully noted that photoablation techniques are commonly used in correcting vision (eg. Laser-Assisted *In Situ* Keratomileusis or LASIK) and thus the use of an excimer laser for our study closely approximates the current clinical practices.

5. Conclusions

The elastic modulus of each layer examined in the rabbit cornea is unique and related to its intrinsic structure. The rabbit cornea is markedly softer than the human cornea primarily due to differences in collagen fiber arrangement and spacing. Keratoprosthetics that incorporate mechanical properties from one species may behave differently in another species with a different corneal elastic modulus. Knowledge of the mechanical properties of each corneal layer is a crucial step in the design of improved substrates that mimic the cellular environment for investigating corneal wound healing *in vitro*. Finally, though not yet critically evaluated, the optimal biophysical attributes of the culture environment for the study of corneal stromal cells behaviors may vary with the species being investigated.

Supplementary Material

Refer to Web version on PubMed Central for supplementary material.

Acknowledgments

The authors thank Dr. Julie Last and JL Analytics as well as Bradley Shibata, Rebecca Seraphin and Sarah DeRemer for assisting with this study. This work was funded by the National Institutes of Health National Eye Institute KO8EY021142 (SMT), R01EY019970 (CJM), R01EY016134 (CJM), P30EY12576 (UC Davis) and an unrestricted gift from Research to Prevent Blindness (UC Davis).

References

1. Last JA, Liliensiek SJ, Nealey PF, Murphy CJ. Determining the mechanical properties of human corneal basement membranes with atomic force microscopy. *Journal of Structural Biology*. 2009; 167:19–24. [PubMed: 19341800]
2. Last JA, Thomasy SM, Croasdale CR, Russell P, Murphy CJ. Compliance profile of the human cornea as measured by atomic force microscopy. *Micron*. 2012; 43:1293–1298. [PubMed: 22421334]
3. Wollensak G, Iomdina E. Long-term biomechanical properties of rabbit cornea after photodynamic collagen crosslinking. *Acta Ophthalmol*. 2009; 87:48–51. [PubMed: 18547280]
4. McKee CT, Last JA, Russell P, Murphy CJ. Indentation versus tensile measurements of Young's modulus for soft biological tissues. *Tissue Eng Part B Rev*. 2011; 17:155–164. [PubMed: 21303220]
5. Abrams GA, Schaus SS, Goodman SL, Nealey PF, Murphy CJ. Nanoscale topography of the corneal epithelial basement membrane and Descemet's membrane of the human. *Cornea*. 2000; 19:57–64. [PubMed: 10632010]
6. Reichard M, Hovakimyan M, Wree A, Meyer-Lindenberg A, Nolte I, Junghans C, et al. Comparative in vivo confocal microscopical study of the cornea anatomy of different laboratory animals. *Current eye research*. 2010; 35:1072–1080. [PubMed: 20961216]
7. Hermann LR. Elasticity equations for incompressible and nearly incompressible materials by a variational theorem. *AIAA Journal*. 1965; 3:1896–1900.
8. Winkler M, Chai D, Kriling S, Nien CJ, Brown DJ, Jester B, et al. Non-Linear Optical Macroscopic Assessment of 3-D Corneal Collagen Organization and Axial Biomechanics. *Invest Ophthalmol Vis Sci*. 2011
9. Last JA, Russell P, Nealey PF, Murphy CJ. The applications of atomic force microscopy to vision science. *Invest Ophthalmol Vis Sci*. 2010; 51:6083–6094. [PubMed: 21123767]
10. Abrams GA, Bentley E, Nealey PF, Murphy CJ. Electron microscopy of the canine corneal basement membranes. *Cells Tissues Organs*. 2002; 170:251–257. [PubMed: 11919413]
11. McKee CT, Wood JA, Shah NM, Fischer ME, Reilly CM, Murphy CJ, et al. The effect of biophysical attributes of the ocular trabecular meshwork associated with glaucoma on the cell response to therapeutic agents. *Biomaterials*. 2011; 32:2417–2423. [PubMed: 21220171]
12. Shively JN, Epling GP. Fine structure of the canine eye: cornea. *Am J Vet Res*. 1970; 31:713–722. [PubMed: 5437109]
13. Bueno JM, Gualda EJ, Artal P. Analysis of corneal stroma organization with wavefront optimized nonlinear microscopy. *Cornea*. 2011; 30:692–701. [PubMed: 21242785]
14. Elsheikh A, Wang DF, Pye D. Determination of the modulus of elasticity of the human cornea. *Journal of Refractive Surgery*. 2007; 23:808–818. [PubMed: 17985801]
15. Fisher RF. The Influence of Age on Some Ocular Basement-Membranes. *Eye-Transactions of the Ophthalmological Societies of the United Kingdom*. 1987; 1:184–189.
16. Wood JA, McKee CT, Thomasy SM, Fischer ME, Shah NM, Murphy CJ, et al. Substratum compliance regulates human trabecular meshwork cell behaviors and response to latrunculin B. *Invest Ophthalmol Vis Sci*. 2011; 52:9298–9303. [PubMed: 22064990]

17. Wood JA, Shah NM, McKee CT, Hughbanks ML, Liliensiek SJ, Russell P, et al. The role of substratum compliance of hydrogels on vascular endothelial cell behavior. *Biomaterials*. 2011; 32:5056–5064. [PubMed: 21501863]
18. Thomasy SM, Wood JA, Kass PH, Murphy CJ, Russell P. Substratum stiffness and latrunculin B regulate matrix gene and protein expression in human trabecular meshwork cells. *Invest Ophthalmol Vis Sci*. 2012; 53:952–958. [PubMed: 22247475]
19. Nogradi A, Hopp B, Revesz K, Szabo G, Bor Z, Kolozsvari L. Atomic force microscopic study of the human cornea following excimer laser keratectomy. *Exp Eye Res*. 2000; 70:363–368. [PubMed: 10712822]
20. Chen SS, Humphrey JD. Heat-induced changes in the mechanics of a collagenous tissue: pseudoelastic behavior at 37 degrees C. *Journal of biomechanics*. 1998; 31:211–216. [PubMed: 9645535]
21. Venugopalan V, Nishioka NS, Mikic BB. The thermodynamic response of soft biological tissues to pulsed ultraviolet laser irradiation. *Biophysical journal*. 1995; 69:1259–1271. [PubMed: 8534796]

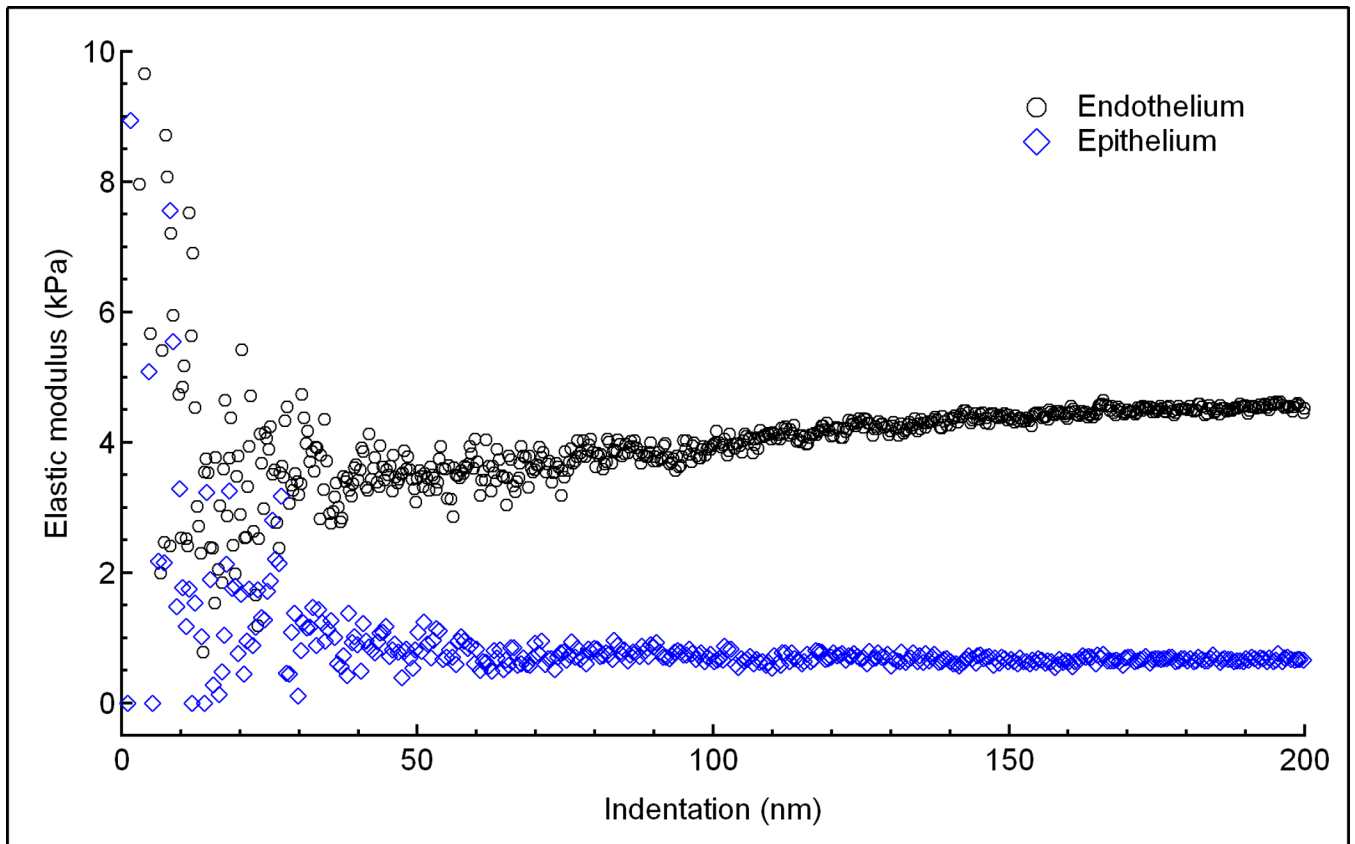


Fig 1.

A plot of elastic modulus versus indentation depth for the endothelium (black circles) and epithelium (blue diamonds). A gradual increase in elastic modulus occurred at indentation depths greater than 100 nm for the endothelium. No change in elastic modulus occurred from indentation depths of 50 to 200 nm for the epithelium.

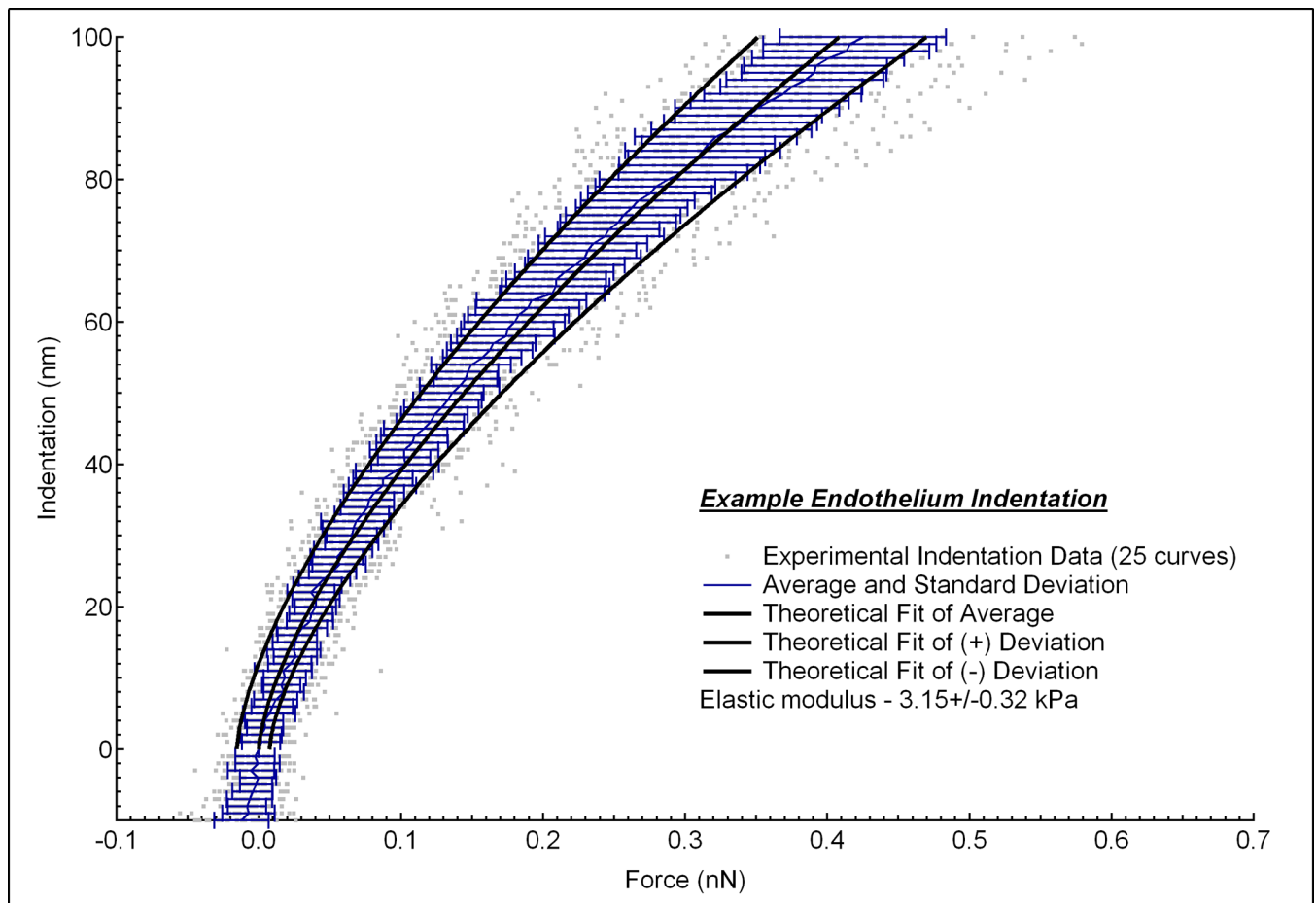


Fig 2.

Indentation vs. force curves measured at 5 positions on the endothelium from one rabbit. At each position, 5 force curves were measured (gray dots). The average and standard deviation of these 25 curves were calculated at each indentation depth (blue lines). From this data, a single curve of the fitted average and two additional curves of the positive and negative standard deviations were generated (black lines). Linear least-square fits of the data using the Hertz model was then performed to the elastic region of the average, positive and negative standard deviations to give an elastic modulus of 3.15 ± 0.32 kPa.

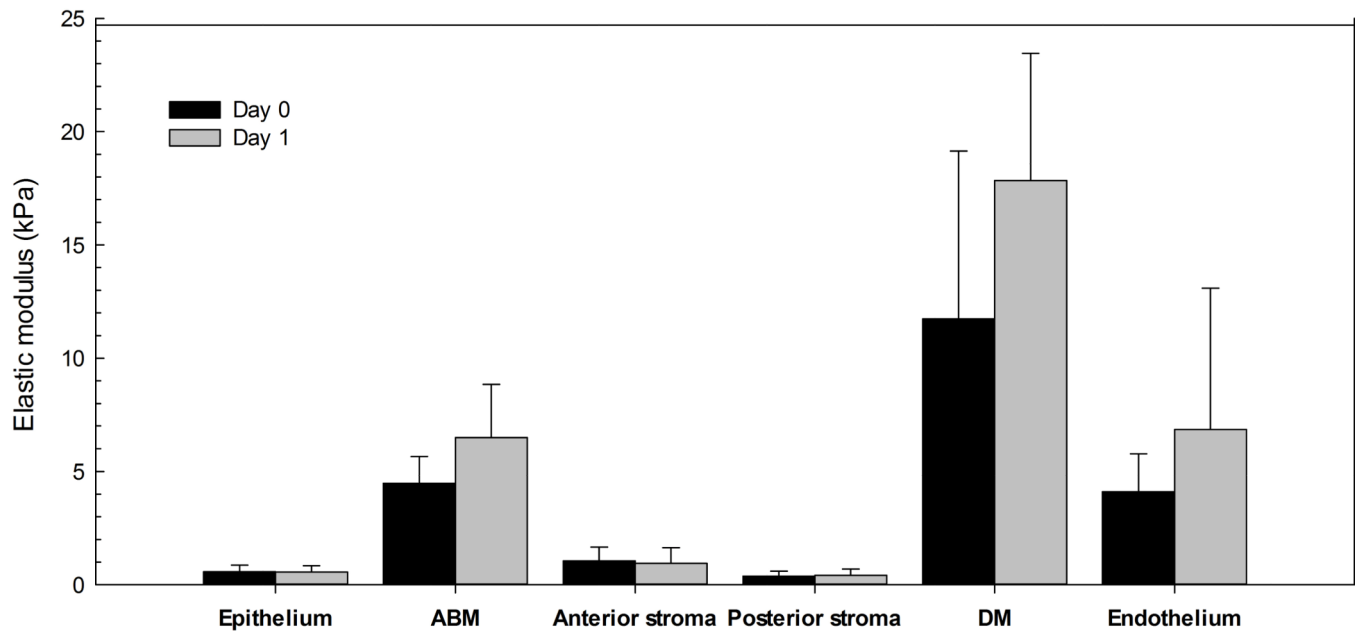


Fig 3. Elastic modulus results for the rabbit corneal epithelium, anterior basement membrane (ABM), anterior stroma, posterior stroma, Descemet's membrane (DM) and endothelium ($n = 3$ /corneal layer) where each cornea was randomly assigned to incubate in Optisol for <2 h (day 0) or 24 h (day 1).

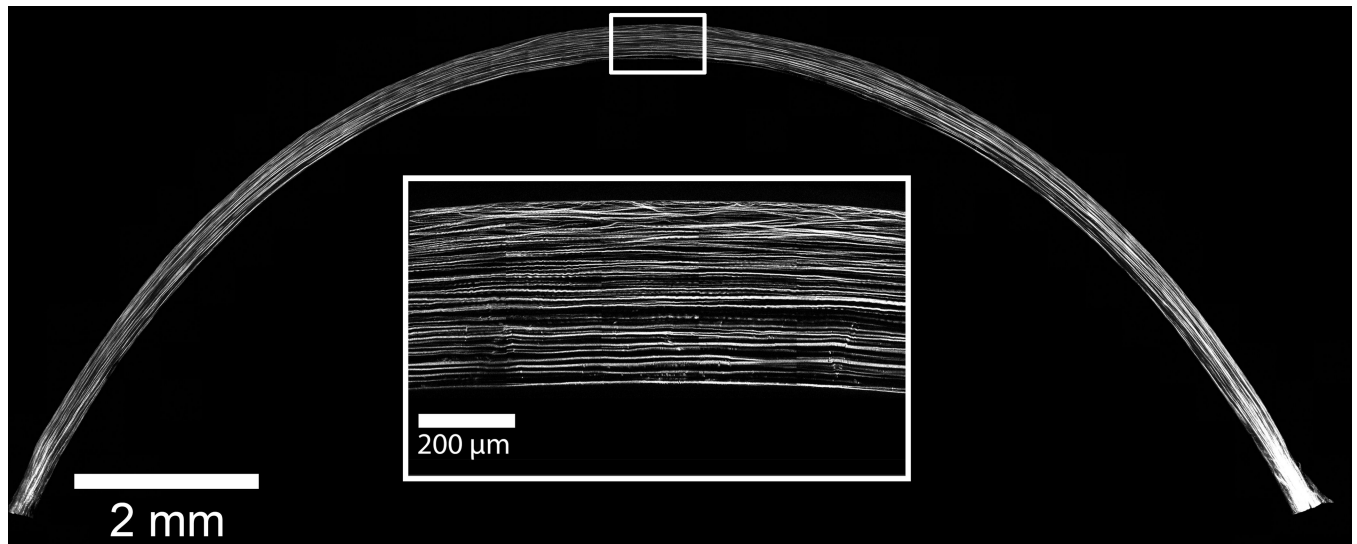


Fig 4.

The parallel arrangement of large, widely separated collagen fibers is the dominant organizational feature of the rabbit cornea as demonstrated in this low resolution ($0.88 \mu\text{m}/\text{pixel}$), single-plane HRMac image of a $300 \mu\text{m}$ vibratome section from the central corneal meridian. Heterogeneity in collagen fiber interactions is only present within the axial anterior cornea as demonstrated in this high-resolution ($0.44 \mu\text{m}/\text{pixel}$) single-plane region of the central rabbit cornea (inlay).

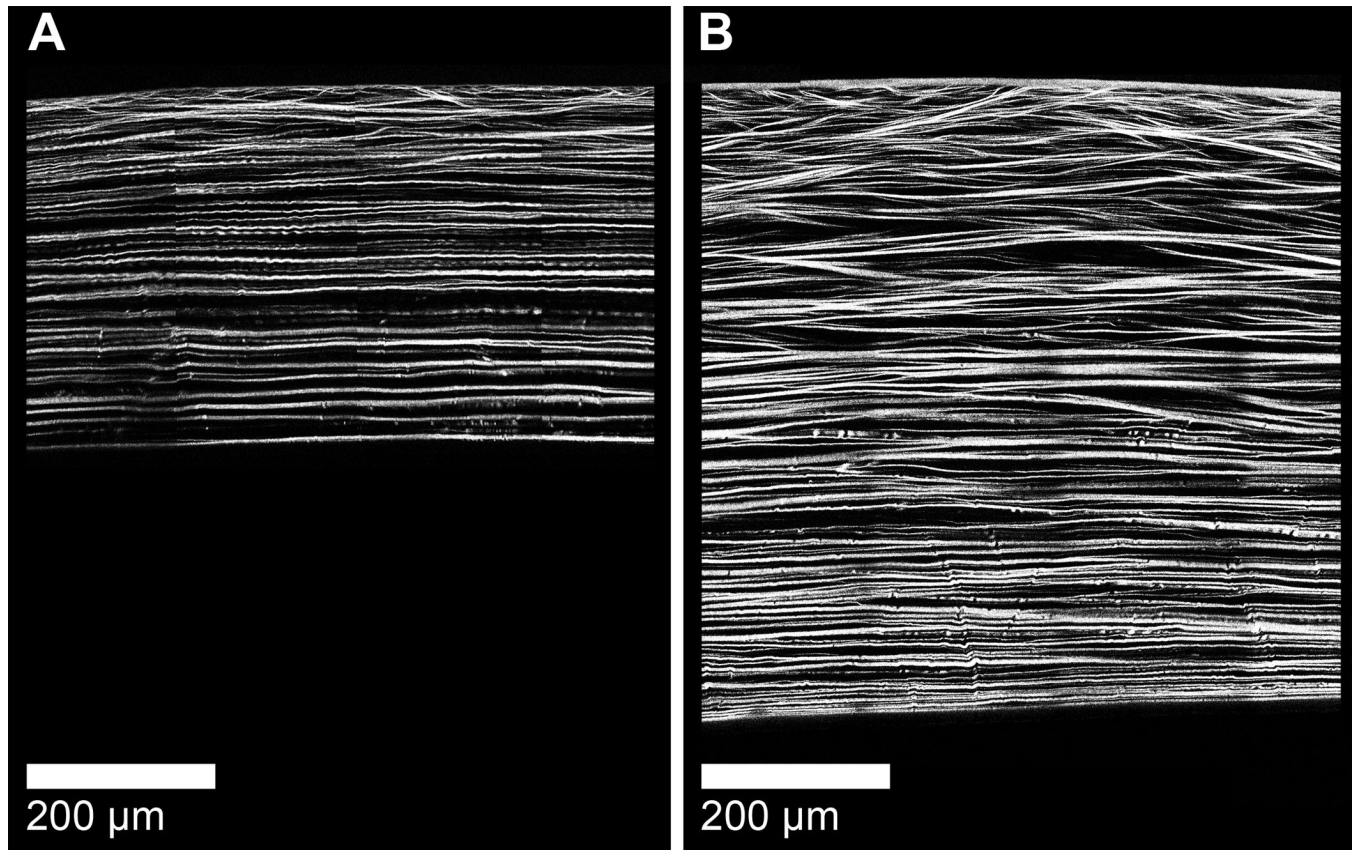


Fig 5. The three-dimensional collagen organization of the rabbit cornea (A) dramatically differs from the human cornea [8] (B). Note that the bulk of the rabbit cornea exhibits parallel arrangement of collagen fibers with collagen intertwining present only in the anterior aspect. In contrast, extensive collagen fiber intertwining is present within the anterior 80% of the human cornea. In the rabbit cornea, collagen fibers are also less densely packed in comparison to the human cornea.